FLUID-STRUCTURE-INTERACTION SIMULATION OF PASSIVE AIR BLAST SAFETY VALVES

Christian Jenni[1], Tim Altorfer[1], Mirco Ganz[1], Sven Düzel[2], Lorenz Brenner[3], André Zahnd[3], Frank Tillenkamp[1]

[1] Zurich University of Applied Sciences (ZHAW), Institute of Energy Systems and Fluid Engineering (IEFE), Technikumstrasse 9, CH-8401 Winterthur;
[2] Zurich University of Applied Sciences (ZHAW), Institute of Mechanical Systems (IMES), Technikumstrasse 9, CH-8401 Winterthur;
[3] Federal Department of Defence, Civil Protection and Sport (DDPS), Federal Office for Civil Protection (FOCP), Spiez Laboratory, Austrasse, CH-3700 Spiez.

Key words:

civil protection, safety valve, blast wave, numerical simulation, experimental investigation

ABSTRACT

Protective structures are usually equipped with ventilation systems, where passive air blast safety valves are important components in the latter. In case of an explosion outside the structure, their purpose is to substantially reduce the occurring blast loading. This assures the protection of human individuals as well as technical installations inside the structure. At the present date, the behaviour of such safety valves is mostly characterized by means of experimental tests in a shock tube or with small explosive loads. In order to gain further insights into the behaviour of the various safety valve closing mechanisms and to support novel developments for modern civil protection systems as well as the error analysis, additional methods are required.

For this reason, this paper presents a practice-oriented procedure, with the aim to obtain the full structural response and blast pressure leakage of passive air blast safety valves by fluid-structure-interaction (FSI) simulations. This comprises three main steps, where first of all potential software solutions have been investigated by means of expert knowledge and literature research. As a second step after the initial theoretical assessment, two different software pairs were tested by carrying out indirectly coupled numerical simulations, i.e. implementing the safety valve as a moving rigid body in the fluid dynamic analysis after the structural assessment. The most promising software pair has been then applied to perform fully coupled FSI simulations. Ultimately, the procedure is exemplified with existing safety valves as a case study.

In comparison to the experimental results, good agreement was achieved with both, indirectly and fully coupled simulations, when analysing the pressure-time history of the blast pressure leakage. However, it was observed, that two-way coupled simulations performed superior considering the closing behaviour and arrival time of the residual blast wave. This might be explained by the fact that the full structural response as well as the corresponding effects on the fluid flow are considered. Furthermore, the closing time was confirmed by high-speed camera registrations of the safety valve during blast loading.

INTRODUCTION

Air blast safety valves are typically installed in protective structures or industrial buildings at the air inlet or outlet. They consist essentially of a valve body, a closing mechanism and a structure, e.g. tension springs, to hold the latter in place during ventilation operation. In the event of an explosion nearby, the safety valve must close instantaneously upon arrival of the blast wave in order to reduce the pressure load inside the structure to a minimum. This assures the protection of people as well as technical installations. At the Spiez Laboratory, passive air blast safety valves are tested in shock tubes, where the blast pressure leakage is characterised in terms of residual pressure-time histories downstream of the valve. With this method, only a post-mechanical analysis of the assessed valve is feasible. However, in order to support new developments for modern civil protection systems as well as failure analysis, methods are required to characterise the safety valve behaviour during blast loading. Since in-situ measurements during shock tube experiments are challenging and with the advances in computer simulations in the last couple of years, Fluid-Structure-Interaction (FSI) simulations appear to be the state of the art technique to gain further detailed insight into the behaviour of different safety valve closing mechanisms.

In FSI simulations, it can be distinguished between a one- and two-way coupling method. In the former, pressure forces are transferred from the fluid-dynamic to the structural solver, where the specimen deformation is computed. No deformation of the geometry is transferred back to the fluid-dynamic solver, and therefore, this method is usually only reasonable if the deflection exhibits a minor effect on the flow field. In contrast, two-way coupling approaches additionally modify the fluid domain with respect to the computed specimen deformation at each time step. Consequently, the two-way coupling method is mandatory when considering safety valves or other components subjected to blast loads, since large deformations occur. Different studies have addressed the issue of FSI simulations of highly deforming geometries. For example, the fluid-structure interaction of clamped steel plates in a shock tube was examined by Aune et al. [1]. An uncoupled and coupled approach was applied for the computation of the dynamic response of the plates as well as the pressure distribution. While a minor difference between the approaches was observed for lower pressure magnitudes, fully coupled FSI simulations are necessary if larger blast loads are considered. Li et al. carried out experimental as well as numerical analyses of concrete-filled steel tubes when subjected to blast loads generated by a cuboidal TNT charge of 200 g within at a scaled distance of 0.079 to 0.175 $m/kg^{1/3}$ [2]. The FSI simulations predicted the observed damage pattern of the tubes with a good accuracy, where a deviation of the simulated buckling depth from the measurements of around 18% was revealed. Similarly, other studies handle the fluid-structure interaction and structural response of different components to blast loads, e.g. an ISO container [3], underwater ductile beams [4] or a flexible cylinder [5].

In this context of FSI simulations, the present work presents a practice-oriented procedure to simulate the structural response and blast pressure leakage of passive air blast safety valves, where the focus lies on fully coupled FSI simulations. The presented method is exemplified with two different types of safety valves at different pressure magnitudes. Additionally, experimental investigations are performed on a shock tube test rig in order to validate the simulation results.

INVESTIGATED PASSIVE AIR BLAST SAFETY VALVES

Figure 1 presents the investigated safety valves. The first (see Figure 1a) consists principally of a rectangular steel body (①) with flexible steel flaps (②) as closing mechanism, which are

deformed during the blast loading and close the airflow path. The second investigated safety valve (see Figure 1b) comprises a circular steel body (①), a half-spherical steel shell (②) as closing mechanism which is held in place by tension springs (③) in ventilation operation and a perforated steel cylinder as pressure reducer (④). Safety valves 1 and 2 are designed and investigated for a reflected pressure of 3 and 40 bar, respectively.

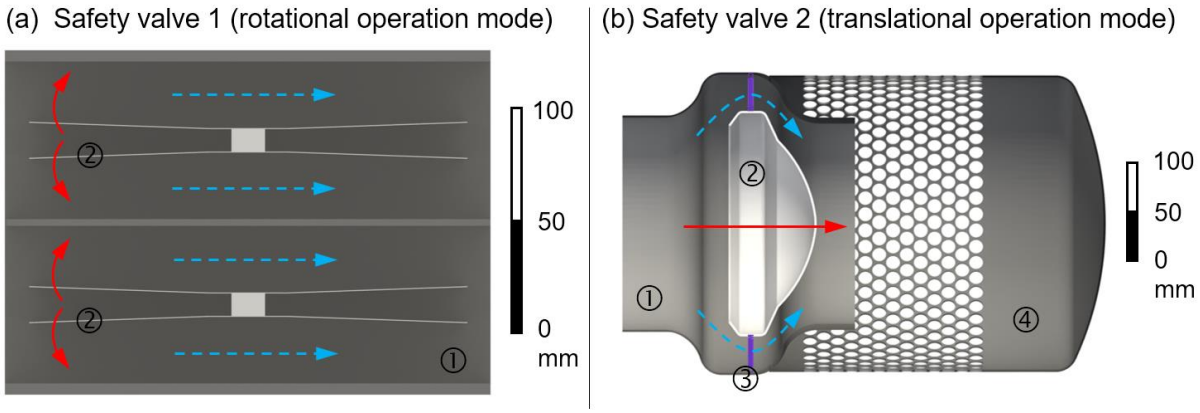

Figure 1: 3D models of the investigated passive air blast safety valves in a vertical cut: (a) rotational and (b) translational operation mode of the closing mechanism. Blue arrows show the airflow path in ventilation operation, where the red arrows indicate the closing mechanism behaviour under blast loading (adapted from Jenni et al. [6] / CC BY-NC 4.0).

SHOCK TUBE TEST RIG

Figure 2 shows a simplified schematic of the shock tube setup applied in the present work. It consists principally of a driver and driven section as well as the measuring section. The safety valve is mounted on an adapter flange at the end of the driven section. Two measuring locations are present, on the one hand to control the incident load (ML1) and on the other hand to monitor the blast pressure leakage (ML2). In order to generate a blast wave, a diaphragm initially separates the driver and driven section. Subsequently, the pressure in the driver section is increased until the burst pressure is reached, i.e. the diaphragm ruptures. This implies a change in fluid state variables (pressure, density, etc.) at the interface and consequently, a pressure wave propagates towards the safety valve. Since two different load levels are being investigated, two shock tube configurations are applied, the specifications of which are listed in Table 1.

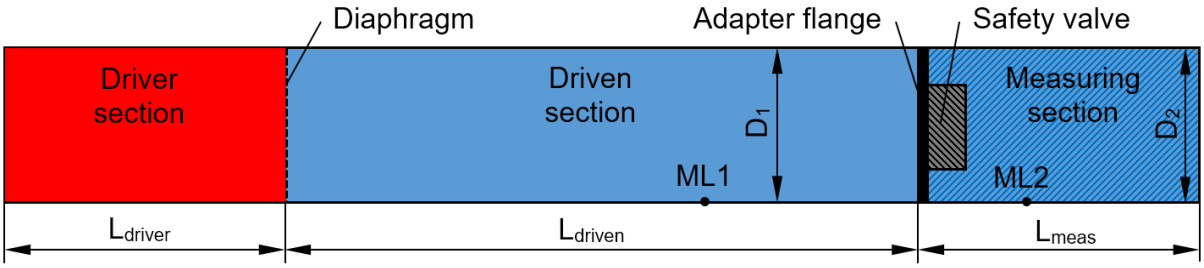

Figure 2: Simplified schematic of the shock tube setup with the driver section (initially at high pressure), driven and measuring section (initially at ambient pressure). Pressure sensors are mounted at measuring location 1 (ML1) and measuring location 2 (ML2) to register the incident and residual pressure with respect to time, respectively.

Table 1: Overview of the applied shock tube configurations.

	Configuration 1	**Configuration 2**
Safety valve no.	1	2
Ambient temperature (reference)	293.15 K	
Ambient pressure (reference)	0.945 bar	
Driver section initial pressure	4.4 bar (relative)	40 bar (relative)
Driven / measuring section initial pressure	0 bar (relative)	
Driver section fluid	Air	Helium
Driven / measuring section fluid	Air	
Driver section length L_{driver}	3 m	0.645 m
Driven section length L_{driven}	15.37 m	4.73 m
Measuring section length L_{meas}	4.04 m	2 m
Driver / driven section diameter D_1	0.486 m	0.212 m
Measuring section diameter D_2	0.486 m	0.43 m

PRELIMINARY WORK

Simulating short-time dynamic phenomena is well known to be a challenging task in numerical fluid-dynamic as well as structural analyses. With the aim of developing a practice-oriented procedure and not being restricted from the start, a comprehensive literature review with regard to FSI simulations and corresponding software, i.e. computational fluid dynamic (CFD) and computational structural dynamic (CSD) tools as well as coupling interfaces, was carried out. For an initial assessment of the possible software solutions, different criteria (e.g. implemented numerical models, mesh generation, availability, usability, etc.) were defined and for each a corresponding weighting factor and degree of target fulfilment was specified. Subsequently, each software was evaluated by experienced users and if not possible, by means of software documentation or research papers. After an initial exclusion procedure, the remaining tools were evaluated with a pairwise comparison, where two different software pairs were chosen for the further procedure.

After the theoretical assessment, simplified simulations tests were carried out. The CFD and CSD tools were used to simulate the empty shock tube and the safety valve mechanism independently from each other, which was successful for every test case. Following, indirectly coupled simulations were performed. In this case, the fluid flow over the whole blast period in the complete shock tube setup, including the safety valve with a fixed closing mechanism, is first simulated. Subsequently, the pressure-time distribution on the safety valve is transferred to the CSD solver for the structural analysis, which provides the displacement curve of the closing mechanism. The latter is then implemented in the CFD solver as a moving rigid body, where again the whole shock tube setup is simulated. This procedure is repeated until changes in pressure distribution as well as displacement curve are negligible small. The simulations were successful in general, although the software pair ANSYS CFX [7] and ABAQUS [8] encountered problems concerning interface mapping and mesh morphing when complex geometries were considered, which made it impossible to simulate the complete closure of the safety valve [9].

According to the described theoretical and practical evaluation, the CFD software APOLLO Blastsimulator [10] together with the CSD solver LS-DYNA [11] provided the most promising results and were therefore considered for the fully coupled FSI simulations.

SIMULATION PROCEDURE AND METHODS

Figure 3 depicts a flow chart of the proposed simulation procedure to carry out fully coupled FSI simulations of passive air blast safety valves. First of all, after defining the case to investigate, the computation domain is created. In order to reduce the computation time, symmetry conditions may be applied. In the present work, a quarter model is used for both evaluated safety valves.

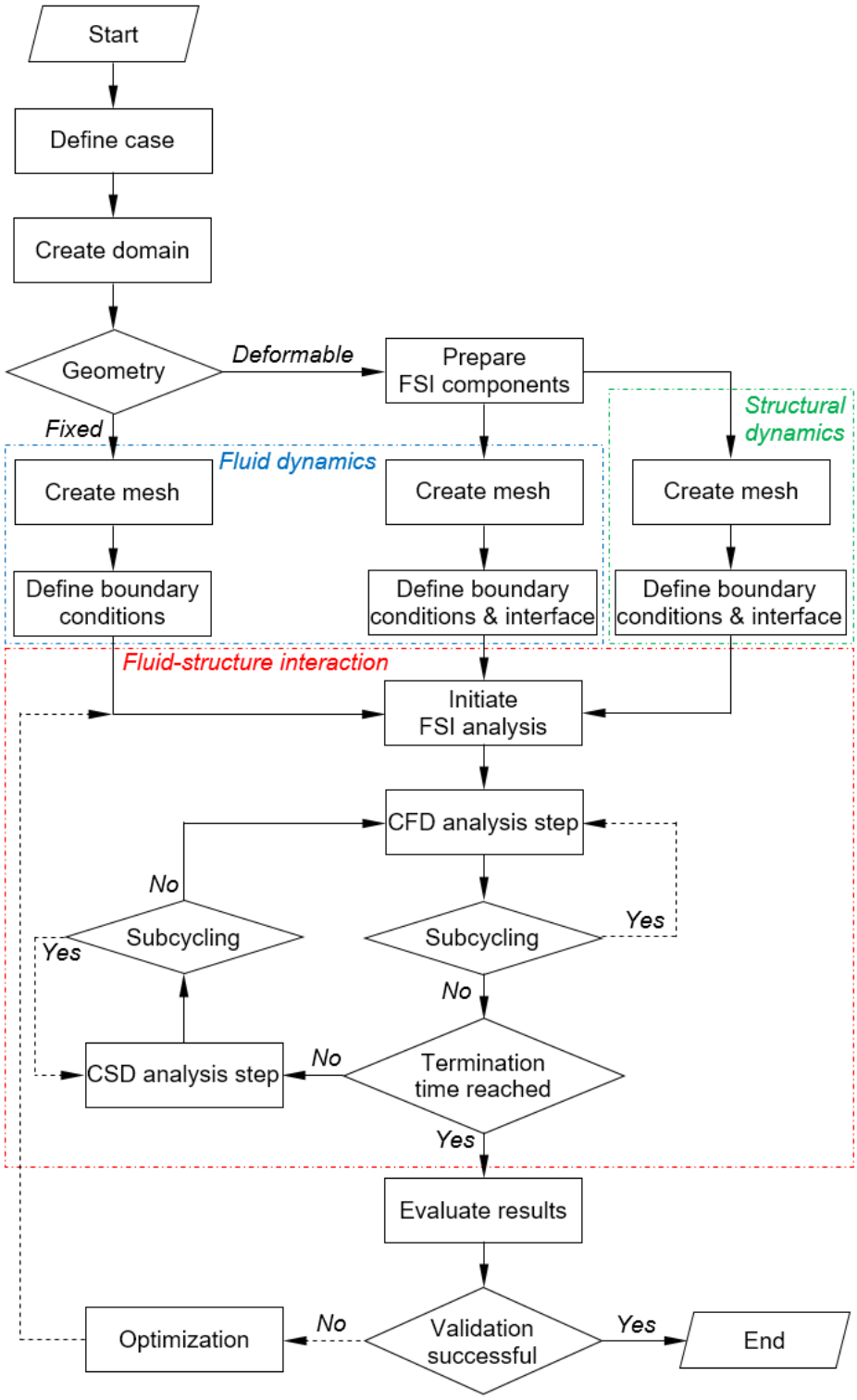

Figure 3: Flow chart of the procedure for fully coupled FSI simulations of passive air blast safety valves.

Subsequently, the Geometry is created, where it has to be distinguished between rigid and deforming components. The rigid parts, e.g. the shock tube walls, are not participating in the coupling procedure and are only present in the fluid dynamic analysis. The deforming components, in the present case the safety valve closing mechanism and body, are both integrated as separate parts in the fluid dynamic as well as structural dynamic solver. In the present study, the shock tube geometry is generated according to the specifications given in Table 1, where the safety valve models are simplified down to the relevant parts. These are then imported via external STL files.

In a next step, the computational grid for the whole domain including the components is generated. Voxel (cube elements) are applied in APOLLO, where a dynamic mesh adaptation (DMA) algorithm is implemented in the software to allow a time-efficient computation. With a mesh sensitivity study, a cell length of 20 mm with a refinement up to 1.25 mm was found to be appropriate for the investigated cases. This results in an average CFD mesh size of approximately 105 and 80 million elements for configuration 1 and 2, respectively. In LS-DYNA, the mesh is generated with linear reduced integrated elements to improve the computational efficiency. To avoid hourglass energy and to ensure the correct physical behaviour of strong bending components, linear fully integrated elements are used in the case of safety valve no. 1. As a result, the CSD mesh contains approximately 52’000 and 32’000 elements for configuration no. 1 and 2, respectively.

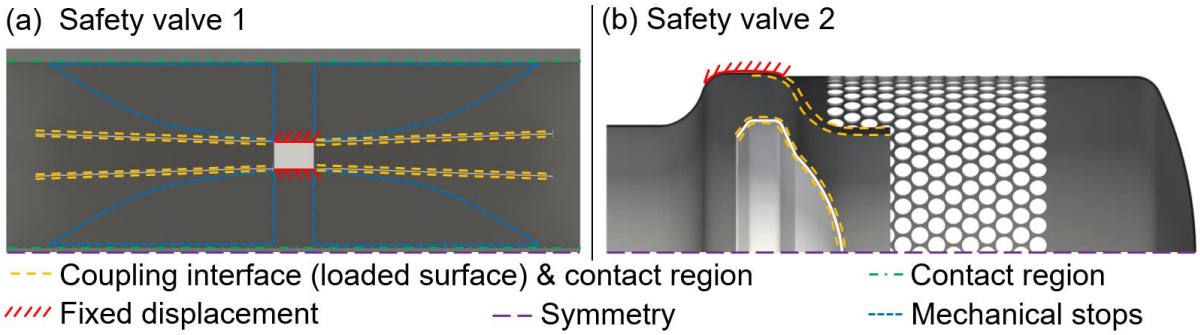

Figure 4: Boundary conditions applied in LS-DYNA for the air blast safety valves: (a) safety valve no. 1 and (b) no. 2 (adapted from Jenni et al. [6] / CC BY-NC 4.0).

After the generation of the computational grid, the boundary and initial conditions as well as the interfaces have to be specified. In the present fluid dynamic analysis, the initial pressure and temperature according to Table 1 is defined, where walls are considered frictionless. The diaphragm is assumed to be burst at the initial time step. An exception is the simulation of configuration 1, since a large shock tube is considered. In order to save computation time, the pressure distribution of an empty shock tube simulation, shortly before the blast wave is reaching the end of the driven section, is mapped as initial condition. The simulated species air and helium are modelled as perfect gases in APOLLO, where for mixtures a mass fraction weighted specific gas constant is applied. Moreover, the boundary conditions for the LS-DYNA simulation are shown in Figure 4. The thin metal sheets in safety valve no. 1 are attached at a centre bar and there fixed in all directions. In safety valve no. 2 the closing mechanism exhibits only one degree of freedom in axial direction, while the others are fixed with respect to the symmetry conditions. The interaction between all safety valve components is modelled using a penalty contact algorithm with a friction coefficient of 0.1. Under the assumption of a bilinear material behaviour, the Cowper-Symonds model is applied in the present work, which allows to consider the strain rate for the elastic as well as plastic regime.

The model coefficients for the steel grades used in the safety valves are estimated based on tensile test data presented in literature [12, 13]. The FSI interface in both analyses, where the load exchange is carried out, is defined as the entire surface of the closing mechanism. APOLLO has implemented an appropriate coupling interface with a corresponding prebuilt subroutine, which can be activated in LS-DYNA using the keyword *USER_LOADING.

Subsequently, the fully coupled simulation is started, first computing one time step in the CFD solver. The pressure distribution on the elements of the coupling interface is then transferred to the CSD solver, where the corresponding deflection and surface velocity is calculated. The latter is provided to the CFD solver and the geometry as well as the computational mesh is adapted in order to start with the computation of the next time step. APOLLO and LS-DYNA are executed synchronized, where the time step size is automatically adapted to meet eventual restrictions given by the numerical scheme or set by the user. So-called subcycling enables disbalanced time steps, meaning the data transfer is skipped for a certain number of iterations. This allows a more time efficient computation, with the drawback of losing computational accuracy. In the present work, 10 subcycles are found to be adequate for the investigated cases. Over the whole simulation, an average time step of 0.15 and 0.18 µs was observed for safety valve no. 1 and 2, respectively.

Ultimately, when the termination time is reached, the numerical data can be analysed and compared with the experimental measurements. If the simulation appears not plausible, further optimization steps might be conducted and the whole simulation repeated.

RESULTS AND DISCUSSION

Safety valve no. 1

Figure 5 depicts the simulated and measured residual overpressure (left y-axis) as well as impulse (right y-axis) in function of the time (x-axis) of safety valve no. 1 at measuring location 2 (compare Figure 2, ML2).

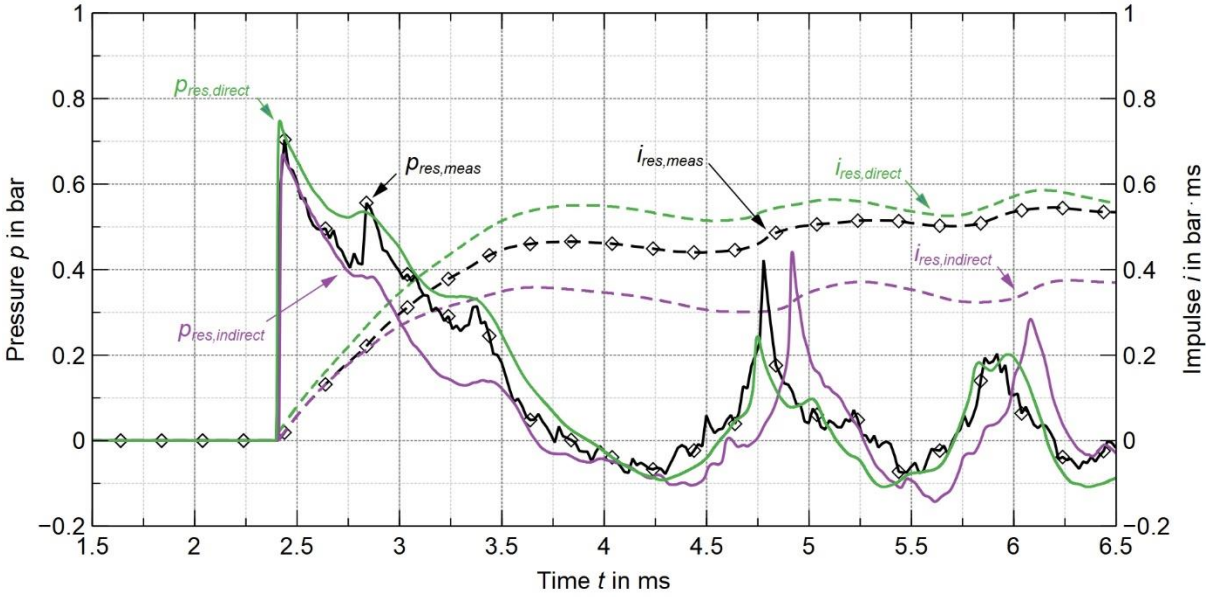

Figure 5: Measured and simulated residual pressure and impulse of safety valve no. 1 at measuring location 2. Purple and green curves represent the indirect and fully coupled FSI simulation, respectively (adapted from Jenni et al. [6] / CC BY-NC 4.0).

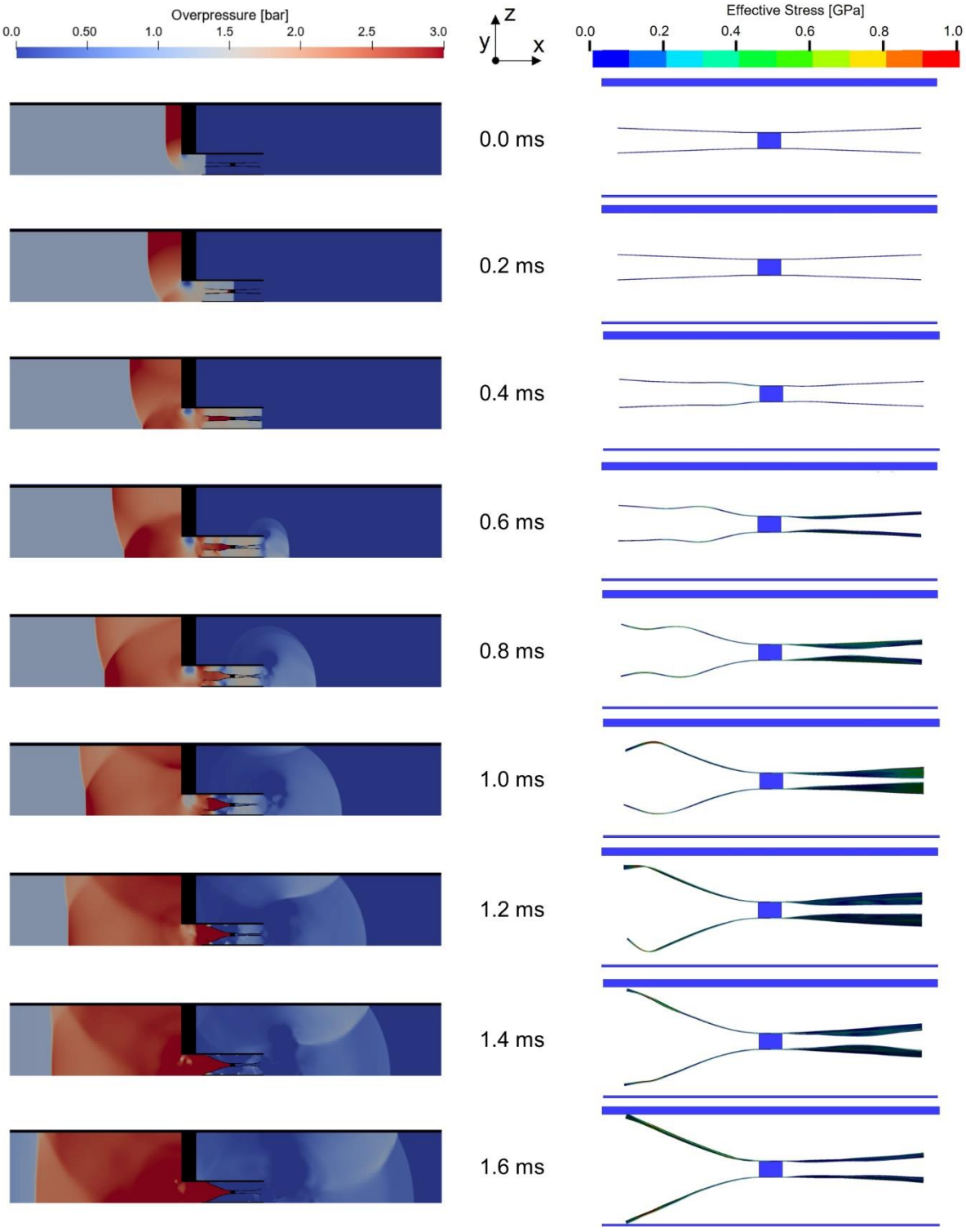

Figure 6: Overpressure contour plot (left) and effective stresses (right) occurring in the closing mechanism of safety valve no. 1 from arrival of the blast wave until closure of the valve (adapted from Jenni et al. [6] / CC BY-NC 4.0).

It is apparent, that the measured peak overpressure of 0.7 bar is adequately predicted with both, the indirect and fully coupled FSI simulations, where a deviation of approximately 7 % is present. Likewise, the first zero crossing of the pressure curve is modelled with a sufficient accuracy. Major differences exist in the whole pressure and impulse time history with the indirectly coupled simulation. The measured overpressure is underpredicted by ca. 0.1 to

0.2 bar between 2.75 to 3.5 ms. Consequently, the maximum impulse is around 0.15 bar·ms lower than in the measurements. Also, the arrival time of both secondary pressure peaks at 4.75 and 6 ms is shifted by around 0.25 ms. One reason for this behaviour might be, that in the indirect FSI simulation the closing mechanism is implemented as a rigid body, which exhibits a strong bending characteristic in reality. Therefore, this changes the fluid flow behaviour significantly. Conversely, the fully coupled simulation predicts the pressure and impulse time history with an acceptable precision, where also the arrival time of the secondary pressure peaks are accurate. Remaining dissimilarities are most likely due to the estimated material model coefficients based on literature, which could be improved by characterising the applied steel grades experimentally.

Furthermore, Figure 6 shows pressure contour plots of the flow field as well as the effective stress in the closing mechanism of safety valve no. 1 from the arrival of the blast wave at 0 ms until valve closure at 1.6 ms.

The functionality of the safety valve mechanism is revealed, where up to 0.2 ms the inner as well as the outer side of the steel flaps are exposed to a side-one overpressure of approximately 1 bar, due to their perpendicular orientation towards the blast wave (movement in positive x-direction). Subsequently, the blast wave is reflected in the inner region of the safety valve at the mounting bar and the pressure is increased. This induces a buckling in the steel sheets which travels in the opposite direction of the blast wave (negative x-direction) towards the flap tips, which is visible from 0.4 to 1.2 ms. Since the flap tips remain almost stationary in the beginning, strain rates and effective stresses larger than 100 1/s and 0.8 GPa are observed, respectively. Interestingly, the steel flaps downstream exhibit a strong bending movement in transversal direction (y-direction). Moreover, pressure wave reflections occur at the shock tube walls downstream of the safety valve, which are also observed in the pressure time history. High-speed camera registrations of the safety valve front confirm the closing time of approximately 1.6 ms, where however the detailed behaviour is not visible. This reveals the importance of fully coupled FSI simulations, where detailed insights of the whole safety valve mechanism are possible.

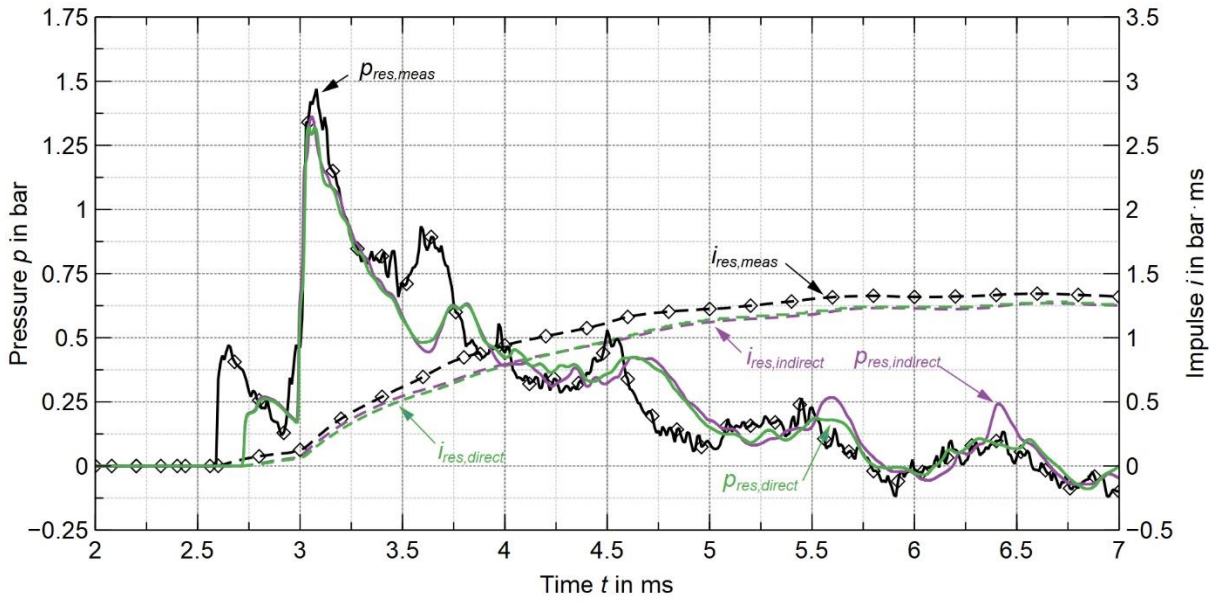

Figure 7: Measured and simulated residual pressure and impulse of safety valve no. 2 at measuring location 2. Purple and green curves represent the indirect and fully coupled FSI simulation, respectively (adapted from Jenni et al. [6] / CC BY-NC 4.0).

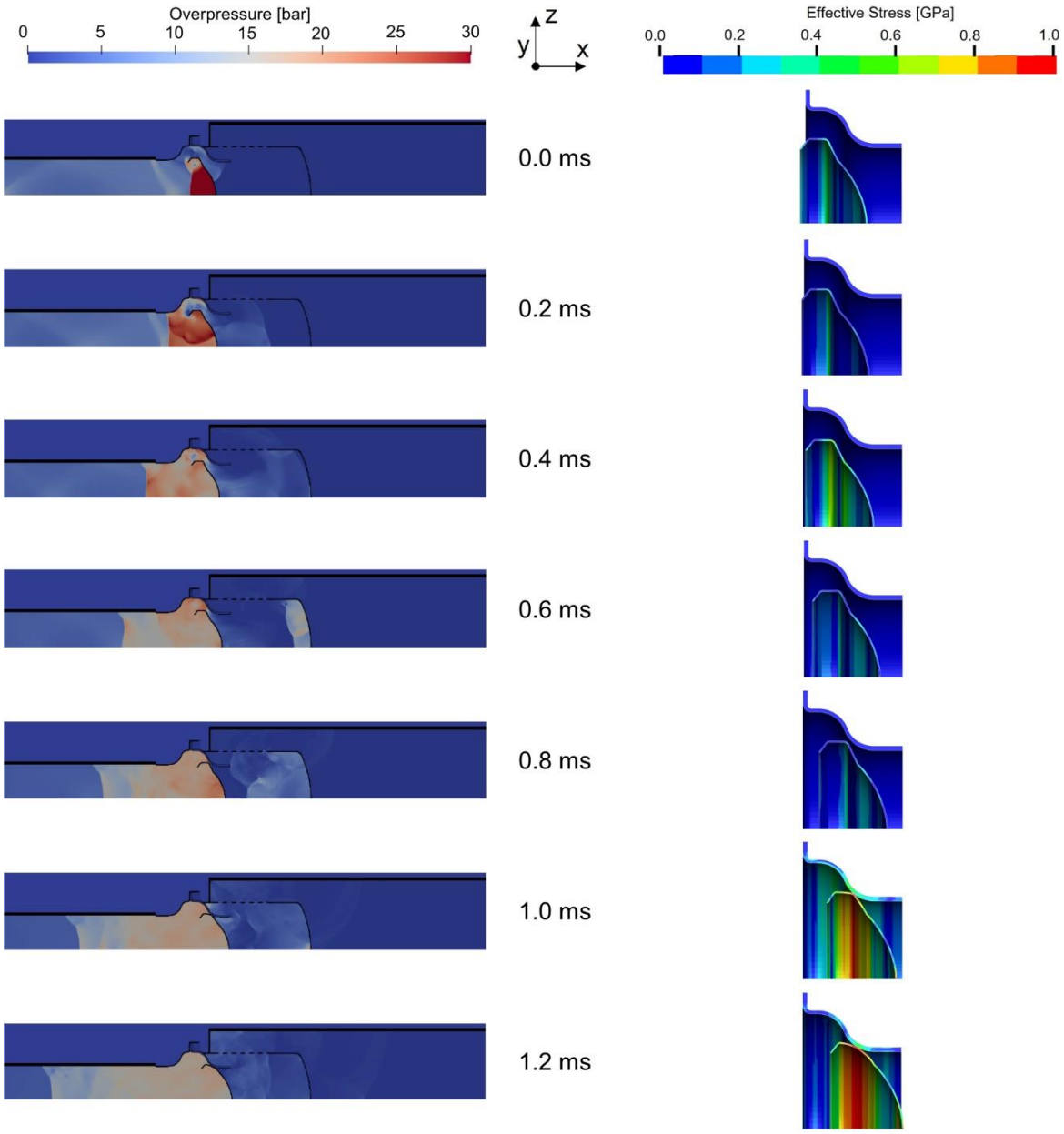

Figure 8: Overpressure contour plot (left) and effective stresses (right) occurring in the closing mechanism of safety valve no. 2 from arrival of the blast wave until closure of the valve (adapted from Jenni et al. [6] / CC BY-NC 4.0).

Safety valve no. 2

Figure 7 depicts the simulated and measured residual overpressure (left y-axis) as well as impulse (right y-axis) in function of the time (x-axis) of safety valve no. 2 at measuring location 2 (compare Figure 2, ML2).

It is visible, that in the case of a translational safety valve mechanism, both FSI approaches deliver similar results. Differences between the measured and simulated pressure curve occur on the one hand in the pressure peaks at 2.75 and 3.6 ms, where in both cases the overpressure is underestimated by approximately 0.25 bar and a shift in arrival time of around 0.25 ms is apparent. Likewise, the pressure decrease at 4.75 ms appears later than in the measurements. Beginning at 5 ms the fully coupled FSI simulation provides a better estimation of the pressure time history compared to the indirect coupling. The cause for these deviations can ultimately not be determined, where possible reasons are the missing integration of the pressure reducer

in the coupling process or the estimated material coefficients similarly to configuration 1. Nevertheless, the peak overpressure, the time until first zero-crossing of the pressure curve and the maximum residual impulse are adequately predicted in comparison to the measurement, with a deviation of around 12, 2 and 7 %, respectively.

Additionally, Figure 8 shows pressure contour plots of the flow field as well as the effective stress in the closing mechanism of safety valve no. 2 from the reflection of the incident blast wave at 0 ms, the valve closure at 0.8 ms and the subsequent squeezing of the hemispherical shell into the body until 1.2 ms.

The contour plot at 0 ms shows the reflection of the incident blast wave, where the pass-through overpressure reaches magnitudes of ca. 12 bar. It takes approximately 0.4 ms to observe any significant movement of the closing mechanism, where at the same time the reflected pressure wave is traveling in negative x-direction upstream of the safety valve. The effect of the pressure reducer is revealed, where a multi-reflection of the pass-through overpressure is visible at 0.6 ms, where magnitudes of up to 25 bar are reached. This secondary pressure wave travels back and forth, with pressure waves at lower magnitude emerging through the perforated area at each time. This most likely explains the pressure fluctuations observed in the pressure time history shown in Figure 7. Shortly after 0.8 ms, the closing mechanism hits the valve body and is pushed into the latter, where significant effective stresses of around 1 GPa are apparent. Such high values would most likely lead to a failure of the hemispherical shell, which was however not observed in post-analyses during the experiments. A possible reason for this overestimation of the stresses is the material model used, which only considers a linear plastic behaviour. Similarly to safety valve no. 1, the carried out FSI simulation delivers additional insights, which are not visible by only considering the measured pressure downstream of the safety valve.

CONCLUSION AND OUTLOOK

The present investigation introduces a practice-oriented procedure to carry out fully coupled FSI simulations of passive air blast safety valves, by applying the software pair APOLLO Blastsimulator and LS-DYNA. The method is exemplified with two different safety valve designs at a lower and higher blast load in the context of shock tube experiments and compared with corresponding experimental results. An adequate agreement between the FSI simulations and pressure measurements downstream of the safety valves is achieved, where the simulations deliver additional insights into the fluid flow as well as specimen behaviour inside the shock tube. According to the findings, optimisation potential exists considering the material model and the applied coefficients. Future work could cover the experimental characterisation of the applied steel grades and the application of a material model that covers also non-linear plastic behaviour. Furthermore, every component of the safety valve could be considered in the coupling process, which however, would most likely result in a major increase in computation time.

ACKNOWLEDGEMENTS

Many thanks go to Michael Riedo and Michel Schilling from Andair AG for providing the test specimens as well as for their in-depth knowledge concerning air blast safety valves. Furthermore, the authors would like to thank all participating experts in the preliminary software evaluation and Angelo Seitz for the support during the shock tube experiments.

REFERENCES

[1] V. Aune et al., “Fluid-structure interaction effects during the dynamic response of clamped thin steel plates exposed to blast loading,” *International Journal of Mechanical Sciences,* p. 106263, 2021.

[2] M. Li et al., “Experimental and numerical study on the behaviour of CFDST columns subjected to close-in blast loading,” *Engineering Structures,* no. 185, pp. 203-220, 2019.

[3] T. Børvik et al., “Response of structures to planar blast loads – A finite element engineering approach,” *Computers and Structures,* no. 87, pp. 507-520, 2009.

[4] Y. Yuan et al., “The influence of deformation limits on fluid-structure interactions in underwater blasts,” *International Journal of Impact Engineering,* no. 101, pp. 9-23, 2016.

[5] V.-T. Nguyen and B. Gatzhammer, “A fluid structure interactions partitioned approach for simulations of explosive impacts on deformable structures,” *International Journal of Impact Engineering,* no. 80, pp. 65-75, 2015.

[6] C. Jenni et al., “Numerical procedure to determine the performance and structural response of passive shock wave safety valves under blast loading,” *International Journal of Protective Structures,* pp. 1-22, 2023.

[7] Ansys® CFX, *Release 18.2,* ANSYS, Inc., 2018.

[8] ABAQUS , *Release 2018,* Dassault Systèmes Simulia Corp., 2018.

[9] L. Brenner et al., “Analysis of pressure drop and blast pressure leakage of passive air blast safety valves: An experimental and numerical study,” *Journal of Loss Prevention in the Process Industries,* no. 75, p. 104706, 2021.

[10] Fraunhofer-Institut für Kurzzeitdynamik (EMI), *APOLLO Blastsimulator Version 2022 Revision 2,* 2022.

[11] Livermore Software Technology, *LS-DYNA Keyword User's Manual R13,* 2021.

[12] B. A. Burgan, “Offshore Technology Report - Elevated temperature and high strain rate properties of offshore steels,” HSE, Norwich, UK, 2001.

[13] C. Schröder et al., “Development of a Stainless Austenitic Nitrogen-Alloyed CrMnNiMo Spring Steel,” *Crystals,* vol. 9, no. 9, p. 456, 2019.